Ion Exchange Column Performance Model for Separation of Zr(IV) and Hf(IV) in Elution Process

Fatemi, Shohreh*[+]; Feizy Zarnagh, Hamid; Kalantari, Masoud; Salehi, Zeynab
Department of Chemical Engineering, Faculty of Engineering, University of Tehran,
P.O. Box 11365-4563 Tehran, I.R. IRAN

ABSTRACT: *A mathematical model of sorption of Zirconium and Hafnium cations mixture and elution of these ions from a cation exchange resin bed is developed. Sulfuric acid is selected as the eluent for selective separation of Zr and Hf in a packed bed of Dowex cation exchange resin. The column model is a dispersed plug flow model,and assumed to consist of randomly packed synthetic and spherical resin beads with constant diameter. The beads are assumed to be porous containing not only active sites on their solid structure but also solution-filled pores. The model incorporates mass transfer resistances including inter and intra-particle effects within the solid and fluid phases. Intra-particle diffusion is treated by employing pore diffusion model. The adsorption phenomena of the cations on the active sites is expressed by the equilibrium relationship characterized by a form of the extended Langmuir equation. The batch experiments are carried out in order to determine Langmuir parameters at equilibrium, and pore diffusivity at transitional conditions. These parameters are used in the dynamic model of adsorption and desorption of the mentioned cations. Unlike a number of earlier models the present mathematical model does not have assumptions such as the linearity of the sorption isotherms, uniform concentration profile in the resin particles and ideal plug liquid flow along the bed. It is found that the present model predicts the breakthrough and chromatographic curves with a fair degree of accuracy. It is concluded that the eluent acid concentration and flow rate of the liquid along the bed are the most two important variables which influence the efficiency of separation.*

KEY WORDS: *Ion exchange resin, Mathematical modeling, Elution process, Zirconium, Hafnium.*

INTRODUCTION

Zirconium metal has historically been used primarily as an internal material for nuclear reactors. Other attractive applications of zirconium are in fabrication of corrosion - resistant chemical process hardware and advanced ceramics as oxides. Particularly, materials used in nuclear reactors are selected for their thermal capture cross-sections, along with other properties. Among other properties, zirconium is selected in nuclear application for its low average thermal neutron capture cross section (approx. 0.18 barns) [1].

The two elements zirconium and hafnium, occur together naturally, but Hf has a substantially larger

* *To whom correspondence should be addressed.*
+ *E-mail: shfatemi@ut.ac.ir*
1021-9986/07/3/61 11/$/3.10

thermal neutron capture cross-section (almost 600 times that of Zr). Naturally occurring crude Zr minerals contain typically about 1 to 5% Hf, thus separation of Zr from Hf allows production of nuclear grade Zr with a lower average thermal neutron capture cross-section by elimination of Hf [2].

Recent efforts to minimize organic wastes (from solvent extraction processes) have proposed aqueous techniques for separation of zirconium and hafnium cations [1]. Ion exchange processes can effectively separate zirconium and hafnium cations. This process in most of its applications uses cylindrical column resin bed in which the feed solution is injected in one end and the effluent is collected at the other. These processes also have found increased applications in a range of diverse fields. Ion exchange is primarily used for the removal of metal ions from sewage in water treating units. Also ion exchange process is used for separation and purification of some protein molecules [2], transition and high valence metals [3, 4].

Mathematical modeling of ion exchange process enables one to evaluate the optimum operating conditions and other important parameters of the ion exchange operation to influence efficiency of separation. Many models have been developed to predict ion exchange performance in a fixed bed of resin particles [5-10].

Two theories can describe multi-component ion exchange; one with macroscopic view and the other a microscopic study; or equilibrium and rate theory, respectively. Equilibrium theory assumes that a local equilibrium exists between the resin and bulk phases and that mass transfer resistance between phases or within the resin beads is negligible. Local equilibrium is not accurate at high flow rates of the fluid. Rate theory, which is based on the rate of diffusion to the exchange site, is more appropriate at low concentrations [5]. Mathematically, equilibrium models run easily and rapidly in simulation programs [6,7]. Rate models, however, challenge the abilities of current computer technology [8-10].

One of macroscopic models such as Thomas model is used for prediction of the concentration-time profiles for the column effluent. This model assumes exchange/ elution process with no axial dispersion and no particle concentration gradient [6]. Some macroscopic models are used for simulation and scale up chromatographic process, in this case; the chromatographic column is considered to be a very large extraction column simplified by discrete mixing-cell model or by continuous axial-dispersion model [7]. In this case again concentration inside the solid phase is uniform and mass transfer rate is fast enough to be ignored.

In microscopic models, kinetic diffusion mechanism inside the resin bead describes dynamic behavior, the species diffuse through the liquid filled pores or/and solid phase and adsorb/exchange according to a linear or nonlinear relationship sorption model [8-10].

A number of earlier models have some assumptions such as linearity of the sorption isotherm and can solve analytically [8]. some of the new references use nonlinear isotherms such as *Langmuir* for single component adsorption [9], and yet others use stoichiometric equilibrium for multicomponent exchanges [10].

We found no reference that used the microscopic model for the exchange of Zr(IV) and Hf(IV) cations in a fixed resin bed, and *Langmuir* isotherm for these mixtures. Additionally the parameters of existing models are not published for sorption of the mentioned cations. The aim of this study is to represent a microscopic model and its effective parameters which incorporate mass transfer terms including intra-particle diffusion and solution phase mass transfer, considering flow abnormalities that arise from axial dispersion. Many experiments are performed in order to determine the equilibrium and kinetic parameters of zirconium and hafnium cations in Dowex 50W-X8 resin. In this study, ion exchange operation is performed in three ways:

1- In batch conditions in which the resin phase and the feed solution of Zr(IV) and Hf(IV) ions are in contact to reach in order to equilibrium.

2- Dynamics of fixed bed, in which the feed solution containing cations are introduced to the resin column to be adsorbed to saturate the adsorbent bed, until the breakthrough curves appear in effluent stream.

3- Elution conditions, in which the resin bed is first loaded by the feed of Zr and Hf cations mixture and then is eluted by suitable eluent.

EXPERIMENTAL

Apparatus

Batch experiments are performed using well stoppered bottles in a constant temperature water bath equipped with a shaker. All experiments are performed at

25 °C constant temperature. Also breakthrough sorption runs and elution of Zr(IV) and Hf(IV) ions are carried out in a glass column with 10 mm internal diameter. The schematic diagram of apparatus is presented in Fig 1. The concentrations of zirconium and hafnium were measured by ICP-AES (Inductively coupled plasma - Atomic Emission Spectroscopy, 150 AX Turbo, Varian).

Materials and standards

Dowex 50WX8 (Mesh size: 100-200, DOW company, with 8% degree of crosslinking) cation exchanger resin was used and the applicability of this adsorbent in hafnium and zirconium separation was evaluated. This resin has the apparent density of 800 kg/m^3, particle porosity of ε_p=0.3 and nominal capacity of about 5 meq/g of dry resin. Other characteristics of this resin are given in table 1.

Resin particles were pretreated by washing with 1 normal sulfuric acid in order to activate particles. Resins in the H^+-form were washed with deionized distilled water in order to remove any excess sulfuric acid.

Hafnium oxychloride ($HfOCl_2.8H_2O$, Aldrich) and zirconium oxychloride ($ZrOCl_2.8H_2O$, Merck) were used to prepare the feed. Stock solutions of these salts were prepared in which each solution contained 1000 mg/l of metal cations (Zr or Hf). Working standards are prepared in 0.1, 0.5, 1 and 1.6 N solutions of sulfuric acid by serial dilution of standard solutions of each cation. All solutions are prepared with deionized distilled water throughout.

Batch experiments

The equilibrium parameters measurements were made by standard shaker tests in which known weights of resin were agitated with Zr(IV) and Hf(IV) solutions of known composition in 0.5 , 1 N and 1.6 N sulfuric acid in a water bath at 25 °C for about 1 hr to reach to equilibrium condition. the samples were then filtered and Zr(IV) and Hf(IV) content in the filtrate were determined by ICP-AES analyzer. Some of these experiments were done for analysis of a single component adsorption and some other runs were performed on two component mixtures.

The experimental equilibrium data of each single component were fitted to *Langmuir* equation to derive the single component equilibrium parameters. The other equilibrium experimental runs of Zr and Hf mixture were carried out to compare the adsorbed amount of cations

Table 1: Properties of ion exchange resin Dowex 50W X8.

Type	Polymeric resin
Material	Sulfonated polystyrene
Counter-ion	H^+
Particle Diameter	120 μm

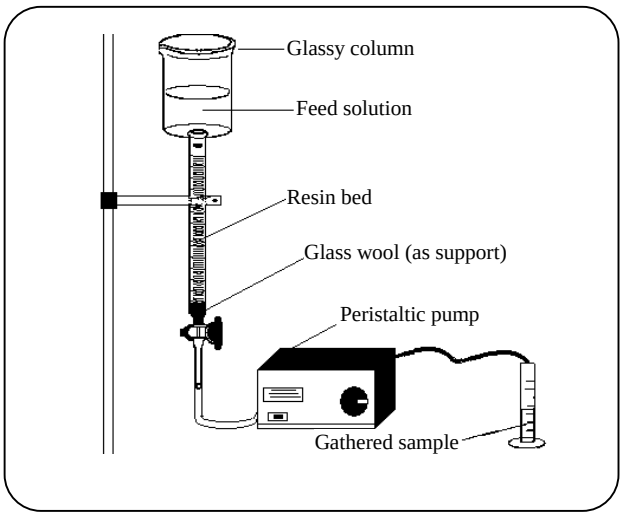

Fig. 1: Schematic diagram of the experimental set up.

with extended *Langmuir* model (Eq. (8)) replacing the single component parameters of adsorption isotherm [11].

Another series of batch experiments were performed in order to evaluate the effective pore diffusion coefficient. It was found that in weak acid solution (0.1 N sulfuric acid) kinetic conditions dominated the equilibrium conditions, it means bulk and resin phases do not reach to the equilibrium in short time, contrast to the higher acid concentrations such as 0.5 and 1 N. The acid concentration of 0.1 N was selected to perform some batch experiments in order to derive concentration-time data for each cation and then evaluate average cation transfer flux to the particle pores by the following equation:

$$V\frac{\partial C_i}{\partial t} = -AJ_i\Big|_{r=Rp} \qquad (1)$$

$$j_i\Big|_{r=Rp} = D_\circ \frac{\partial C_{Pi}}{\partial r}\Big|_{r=Rp} \qquad (2)$$

V is solution volume and A is the total external surface of the particles, Ci is the solution concentration and C_{Pi} is pore concentration at the particle surface which

is assumed equal to the solution concentration at each time ,when there is no film resistance.

The batch experiments were carried out at transitional condition with agitation of the solution, and concentration-time data were obtained for three different initial concentrations of each single component (20 and 40 and 60 ppm). Using *Lump* formulation of each species in solution, the ion transfer flux (J) was derived, and diffusivity was calculated by *Ficks'* equation for each initial concentration then averaging the results [11].

Column bed runs

The column breakthrough measurements were carried out at 25 ^{o}C in a glass column packed with Dowex 50 W X8. A peristaltic pump was used for feeding Zr(IV) and Hf(IV) solutions in different sulfuric acid concentration to the column. The column effluent was sampled at regular intervals and was analyzed by ICP-AES analyzer.

Chromatographic curves were obtained after loading the resin bed with a known concentration and known volume of solution, followed by acid elution. Elution of the loaded resin bed performed in column experimental runs; by sulfuric acid with different concentrations, to achieve a higher efficiency of separation [11,12].

DYNAMIC MODEL

Mathematical modeling for packed bed ion exchange column has two main parts: column model and particle model (included equilibrium model). Following assumeptions are implicit in this model:

- The liquid flow is considered as axial dispersion model and may be characterized by the axial diffusion coefficient.
- The effective pore diffusion coefficient inside the particles is independent to the concentration of ions, because of very low concentrations.
- The adsorption sorption and desorption process of the ions is isothermal, because of low adsorption enthalpies.
- Mass transfer term in the liquid film is represented by a linear relationship.
- The resin bed is homogeneous with uniform porosity.
- The resin particles are spherical and uniform in density and radius and porosity.
- The solid phase is in equilibrium with filled liquid in the pores and the equilibrium model is represented by extended *Langmuir* equation for mixture of cations.

Column model

Consider a fixed and vertical cylindrical bed made up of spherical resin beads. A material balance for each cation in bulk liquid phase yields:

$$\frac{\partial C_i}{\partial t}+\frac{1-\varepsilon}{\varepsilon}\frac{3}{R_p}k_{f,i}(C_i-C_{p,i}\big|_{r=Rp})= \quad (3)$$

$$D_L\frac{\partial^2 C_i}{\partial z^2}-\frac{U_L}{\varepsilon}\frac{\partial C_i}{\partial z}$$

i: Zr or Hf

The first term on the left hand side arises from accumulation of ions in the solution. The second term on the left arises from the effect of film mass transfer on the particle surface. The first term on the right hand is due to axial dispersion of flow and the second one arises from bulk convection. The following boundary and initial conditions were applied for the fixed bed ion exchange column:

$$-D_L\frac{\partial C_i}{\partial z}|_{z=0}=\frac{U_L}{\varepsilon}\left(C_{0,i}-C_i\,|_{z=0}\right) \quad (4)$$

$$\frac{\partial C_i}{\partial z}|_{z=L}=0 \quad (5)$$

$$t=0\Rightarrow C_i=C_{initial} \quad (6)$$

Particle model

The mole balance in resin particles expressed by the following equation:

$$\frac{\partial C_{p,i}}{\partial t}+\frac{(1-\varepsilon_p)}{\varepsilon_p}\frac{\partial q_i}{\partial t}= \quad (7)$$

$$D_{p,i}\left[\frac{\partial^2 C_{p,i}}{\partial r^2}+\left(\frac{2}{r}\right)\frac{\partial C_{p,i}}{\partial r}\right]$$

The term $\partial q_i/\partial t$ on the left side arises from accumulation of ions in the solid resin phase, which is explained by *Langmuir* equilibrium model for mixtures. The extended *Langmuir* isotherm for a mixture of two components is presented as following:

$$q_i=\frac{q_\infty b_i C_{p,i}}{1+\sum_{i=1}^{2} b_i C_{p,i}} \quad (8)$$

Table 2: Parameters of the Langmuir sorption isotherm for single components on Dowex 50W X8 resin at 25 °C.

Cation	0.5 N sulfuric acid		1 N sulfuric acid		1.6 N sulfuric acid	
	q_m (μg/ml)	b (ml/μg)	q_m (μg/ml)	b (ml/μg)	q_m (μg/ml)	b (ml/μg)
Zr (IV)	743	0.110	63	0.108	31	0.02
Hf (IV)	1394	0.530	120	0.500	62	0.052

Thus $\partial q_i/\partial t$ can be replaced by differentiation of Eq. (8) with respect to time such as Eq. (9):

$$\frac{\partial q_i}{\partial t} = \sum_{j=1}^{2} \frac{\partial q_i}{\partial C_{p,j}} \frac{\partial C_{p,j}}{\partial t} \qquad (9)$$

The boundary and initial conditions for the particle model are as follows:

$$\frac{\partial C_{p,i}}{\partial r}|_{r=0} = 0 \qquad (10)$$

$$\varepsilon_p D_{p,i} \frac{\partial C_{p,i}}{\partial r}|_{r=Rp} = k_{f,i}\left(C_i - C_{p,i}|_{r=Rp}\right) \qquad (11)$$

$$t = 0 \Rightarrow C_{p,i} = 0 \qquad (12)$$

Equations (3) and (7) with their respective initial and boundary conditions constitute the model required for the prediction of the dynamics of fixed bed ion exchange. These two equations are bounded together by the boundary condition of Eq. (11). The ion exchange parabolic PDE equations described by the represented model have been solved by finite difference method in this work. The numerical algorithm is presented in appendix.

Column Model Parameters

The axial dispersion coefficient, D_L, is calculated by equation (13) and the liquid film mass transfer coefficient is calculated by equation (14). The effective pore diffusion is related to the molecular diffusion coefficient and tortousity factor, using equation (15) [13]. The physical properties of the solution are similar to water which are substituted into the model equations.

$$\frac{U_L d_p}{\varepsilon D_L} = \left(\frac{0.2}{\varepsilon}\right) + \left(\frac{0.011}{\varepsilon}\right)\left(\frac{\rho d_p U_L}{\mu\varepsilon}\right)^{0.48} \qquad (13)$$

$$\left(\frac{k_f \varepsilon}{U_L}\right)\left(\frac{\mu}{\rho D}\right)^{\frac{2}{3}} = 1.85\left(\frac{\rho d_p U_L}{\mu(1-\varepsilon)}\right)^{-\frac{2}{3}}\left[\frac{(1-\varepsilon)}{\varepsilon}\right]^{-\frac{1}{3}} \qquad (14)$$

for $\dfrac{\rho d_p U_L}{\mu(1-\varepsilon)} < 100$

$$D_p = \frac{D_m}{\tau_o} \qquad (15)$$

RESULTS AND DISCUSSION

Langmuir parameters

Linear regression of the experimental one-component equilibrium data to the *Langmuir* isotherm leads to *Langmuir* model constants with 0.96 and 0.92 correlation coefficient (R^2) for Zr and Hf, respectively. The derived constants are presented in table 2 for different sulfuric acid concentrations.

These equilibrium constants have been used to simulate the two-component extended Langmuir isotherm (Eq. (8)) in 0.5 N sulfuric acid at 25 °C, and the results are compared with experimental data obtained from the equilibrium mixture, such as Fig. 2. It is found that average absolute relative deviations (AARD) are 9% for Zr and 16% for Hf in binary equilibrium adsorption.

Effective pore diffusion coefficients

The diffusion coefficients are evaluated by calculating average ion transfer flux and using concentration gradient, then using tortousity factor of 6 in Eq. (15). The minimum and maximum calculated effective diffusivities with respect to different solution concentrations are presented in table 3. The mean value of $D_p = 8.85 \times 10^{-7}$ cm^2/m is in reasonable agreement with data reported for the the resin exchange of Zr(IV) [14]. Pore diffusion coefficients of zirconium and hafnium ions at the same conditions must be equal because these ions have similar ionic radius.

Breakthrough curves

The column breakthrough experiments were conducted at conditions as reported in table 4. Figs. 3 and 4

are a comparison of the experimental breakthrough curve data with prediction made by the model described above. The figures show that the model is able to predict the breakthrough curves with an acceptable accuracy. Comparison of the two figures reveals the effect of sulfuric acid concentration on the shape of breakthrough curves.

It is observed that kinetic mechanism is dominated with low acid concentrations in the resin bed but in higher acid concentrations saturation of the bed plays the main role. As a result the bed with lower acid concentration (0.5 N) saturates later by the metal cations, and more effective separation is obvious in presence of low sulfuric acid concentration.

Elution process

Finally the resin bed elution experiments were conducted at conditions as reported in table 5. In the elution process the bed is first loaded by a known volume of the solution at the top of the bed, then the eluent is subjected to the column. The elution process is carried out by the solution of sulfuric acid to derive chromatographic curves of Zr and Hf.

Experimental and predicted chromatographic curves are evaluated and compared in Fig. 5. which has employed sulfuric acid as the eluent. This figure indicates that using 1.6 N sulfuric acid can not effectively separate two metal ions but using lower concentration of sulfuric acid (0.5 N) improves the separation efficiency [12]. Theoretically, high concentration of acid causes higher rate of reaching to the equilibrium condition, and because most sites of the cation exchange resin is occupied by hydrogen ions, not by Zr nor by Hf, performance of the resin decreases considerably. In contrast to the higher water acid concentrations, highest separation factor has been observed in batch experiments at 25 °C in presence of 0.5 N sulfuric acid [12], also the dynamic run in Fig. 3 indicates high separation efficiency of Zr from Hf.

Sensitivity analysis

Comparison of breakthrough curves of Fig. 3 and Fig. 4, with different sulfuric acid concentrations in the mobile phase, shows that sulfuric acid concentration has significant effect on the residence behavior of the cations, which was mentioned earlier. It is concluded that lower concentration of sulfuric acid causes higher purity of Zr in the outlet.

Table 3: Effective pore diffusion coefficient for diffusion of zirconium cation in Dowex 50W X8 at 25 ^{o}C.

	$D_P \times 10^{-7}$ (cm^2/s)
Minimum	1.12
Maximum	16.6
Average	8.85

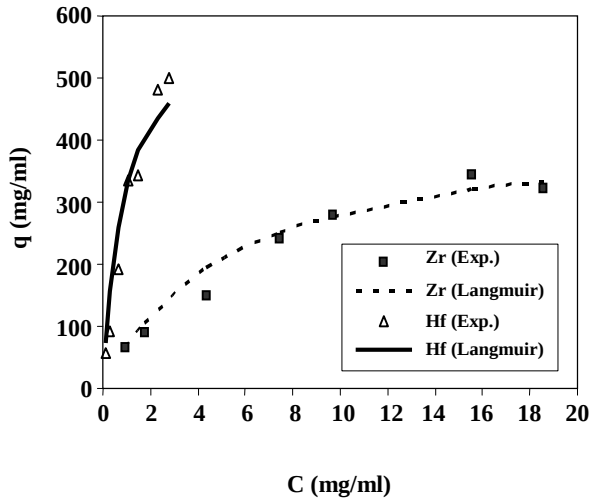

Fig. 2: Experimental and predicted two components equilibrium isotherms for Zr(IV) and Hf(IV) on Dowex 50W X8 at 25 ^{o}C, in 0.5 N sulfuric acid solution.

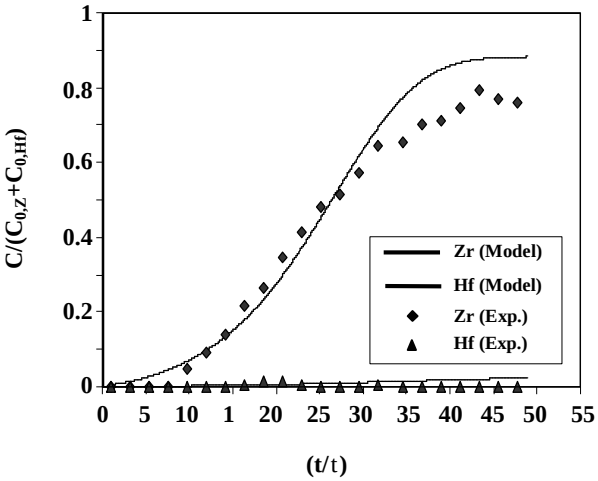

Fig. 3: Comparison of experimental and predicted breakthrough curves (at 25 ^{o}C, 0.5 N Sulfuric acid has been used as mobile phase, other conditions according to table 4).

Table 4: Operating conditions of two component column breakthrough runs in sulfuric acid at 25 °C.

Acid concentration	U_L (cm/s)	Resin weight (g)	$C_{F,Zr}$ (μg/ml)	$C_{F,Hf}$ (μg/ml)	D_L, (cm^2/s)	K_f, (cm/s)
0.5 N	0.013	2.5	19.6	4.2	$7.7x10^{-4}$	$9.5x10^{-4}$
1 N	0.013	7.2	16.0	3.1	"	"

Table 5: Operating conditions of elution of the loaded resin bed by Zr(IV) and Hf(IV) cations at 25 °C.

Eluent	U_L (cm/s)	Resin weight (g)	$C_{injection,Zr}$ (μg/ml)	$C_{injection,Hf}$ (μg/ml)	Volume of injection (ml)
1.6 N Sulfuric acid	0.0080	10	1695	364	2.5

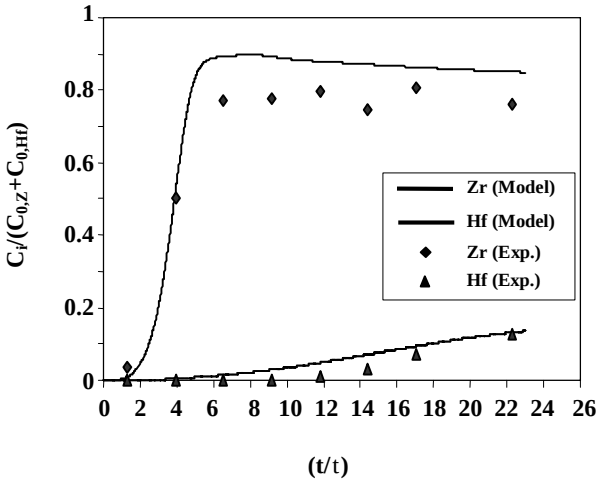

Fig. 4: Comparison of experimental and predicted breakthrough curves (at 25 °C, 1 N Sulfuric acid has been used as mobile phase, other conditions according to table 4).

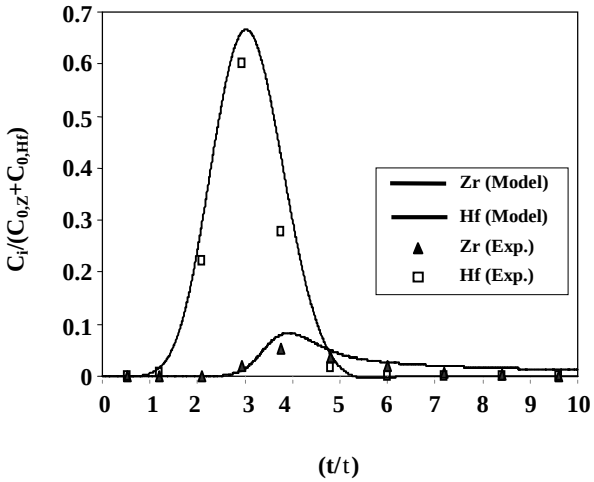

Fig. 5: Comparison of experimental and predicted chromatographic curves at 25 °C, 1.6 N Sulfuric acid has been used as eluent, other conditions according to table 5.

Fig. 6 (a-c), represents running numerical program of the chromatographic curves in different conditions of mobile phase velocity and injection concentrations of Zr(IV) and Hf(IV) at 1.6 N sulfuric acid. Comparison of these varying conditions indicates that liquid velocity and injection concentration of the metal ions are important factors in improving ion exchange performance.

Higher liquid flow rate and higher inlet concentrations of the cations are the worst conditions and show lowest purity of the effluent in Fig. 6a. Lower flow rate and feed concentration shows the capability of the high separation efficiency as Fig. 6c. It is concluded that for effective separation of these cations low liquid velocity is required to reach to high degree of separation, so this procedure could not be used for high capacities of effluents.

CONCLUSIONS

The ion exchange process by Dowex 50W X8 cation exchange resins has shown effective separation of zirconium and hafnium ions at low sulfuric acid concentration (0.5 N), high residence times (more than 10 min) and low cation concentrations (less than 300 ppm) in the present research.

The ion exchange isotherm data of sorption of the cations on these resins can be represented by *Langmuir* two-component isotherm. The equilibrium constants depend on the concentration of the presented sulfuric acid in the feed. Column breakthrough and chromatographic experiments can be simulated by an axial-dispersed flow model accompanied with pore diffusion model inside the resin particle. It was found that the presented model predicts the breakthrough and chromatographic curves

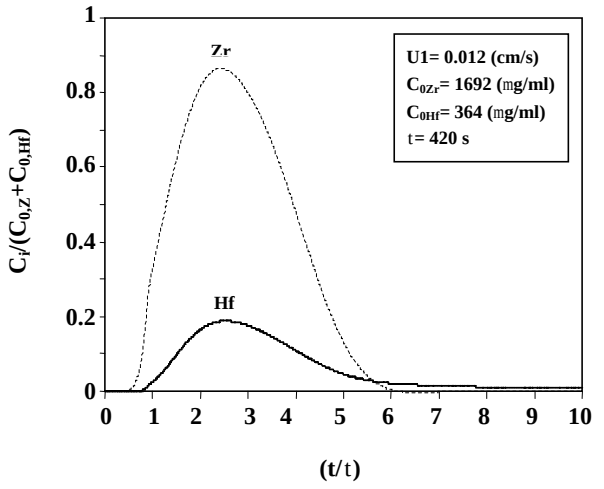

(a)

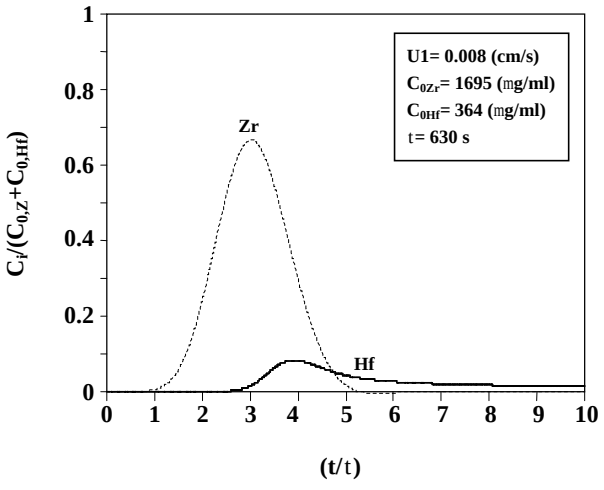

(b)

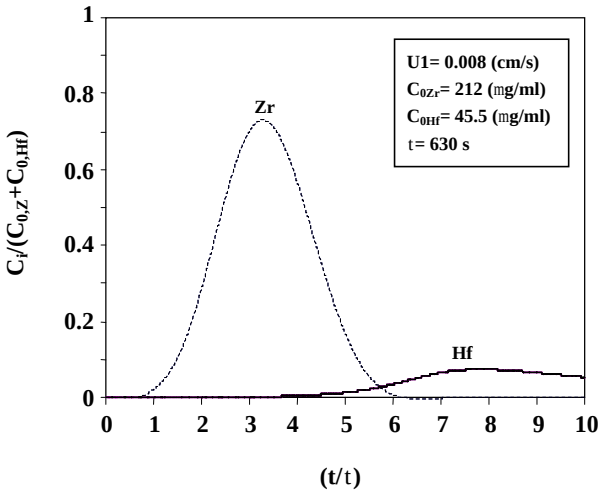

(c)

Fig. 6 (a-c): Model predictions under varying mobile phase velocity and injection concentrations of Zr(IV) and Hf(IV).

with an acceptable degree of accuracy. There was about 4-20% AARD between experimental and predicted data. The experimental and predicted data indicate that concentration of sulfuric acid used as mobile phase, liquid velocity in the ion exchange column and injection concentrations of cations are important parameters in improving separation efficiency.

APPENDIX

Particle Model

For simultaneous solution of particle and bed equations, the solid phase concentration (q_i) was replaced by the function of pore concentration (C_{pj}) using *Langmuir* isotherm for each species as follows:

$$q_{Zr} = \frac{q_{m,Zr} b_{Zr} C_{p,Zr}}{1 + b_{Zr} C_{p,Zr} + b_{Hf} C_{p,Hf}} \quad \text{(A-1)}$$

$$q_{Hf} = \frac{q_{m,Hf} b_{Hf} C_{p,Hf}}{1 + b_{Zr} C_{p,Zr} + b_{Hf} C_{p,Hf}} \quad \text{(A-2)}$$

the term $\partial q_i/\partial t$ in Eq. (7) was substituted by:

$$\frac{\partial q_i}{\partial t} = \frac{\partial q_i}{\partial C_{p,Zr}} \frac{\partial C_{p,Zr}}{\partial T} + \frac{\partial q_i}{\partial C_{p,Hf}} \frac{\partial C_{p,Hf}}{\partial t} \quad \text{(A-3)}$$

The terms $\partial q_i / \partial C_{p,Zr}$ and $\partial q_i / \partial C_{p,Hf}$ are derived from differentiation of *Langmuir* isotherm for each cation; for example if i= Zr :

$$\frac{\partial q_{Zr}}{\partial C_{p,Zr}} = \frac{q_{m,Zr} b_{Zr} \left(1 + b_{Hf} C_{p,Hf}\right)}{\left(1 + b_{Zr} C_{p,Zr} + b_{Hf} C_{p,Hf}\right)^2} \quad \text{(A-4)}$$

$$\frac{\partial q_{Zr}}{\partial C_{p,Hf}} = \frac{-b_{Hf} \times q_{m,Zr} b_{Zr} C_{p,Zr}}{\left(1 + b_{Zr} C_{p,Zr} + b_{Hf} C_{p,Hf}\right)^2} \quad \text{(A-5)}$$

After substitution of A-4 and A-5 in A-3, then in Eq. (7), the following equations are derived for i=Zr:

$$\frac{\partial C_{p,Zr}}{\partial t} + \frac{1}{1 + \left(\frac{1-\varepsilon_p}{\varepsilon_p}\right) \frac{\partial q_{Zr}}{\partial C_{p,Zr}}} \times \quad \text{(A-6)}$$

$$\frac{\left(1-\varepsilon_p\right)}{\varepsilon_p} \frac{\partial q_{Zr}}{\partial C_{p,Hf}} \frac{\partial C_{p,Hf}}{\partial t} = \frac{1}{1 + \left(\frac{1-\varepsilon_p}{\varepsilon_p}\right) \frac{\partial q_{Zr}}{\partial C_{p,Zr}}} \times$$

$$D_{p,i} \left[\frac{\partial^2 C_{p,Zr}}{\partial r^2} + \left(\frac{2}{r}\right) \frac{\partial C_{p,Zr}}{\partial r} \right]$$

$$\frac{\partial C_{p,Zr}}{\partial t}+\frac{1}{F}\frac{(1-\varepsilon_p)}{\varepsilon_p}\times \quad \text{(A-7)}$$

$$\frac{-b_{Hf}\times q_{m,Zr} b_{Zr} C_{p,Zr}}{(1+b_{Zr}C_{p,Zr}+b_{Hf}C_{p,Hf})^2}\frac{\partial C_{p,Hf}}{\partial t}=$$

$$\frac{1}{F}D_{p,i}\left[\frac{\partial^2 C_{p,Zr}}{\partial r^2}+\left(\frac{2}{r}\right)\frac{\partial C_{p,Zr}}{\partial r}\right]$$

function F is shown as the following:

$$F=1+\left(\frac{1-\varepsilon_p}{\varepsilon_p}\right)\frac{q_{m,Zr}b_{Zr}(1+b_{Hf}C_{p,Hf})}{(1+b_{Zr}C_{p,Zr}+b_{Hf}C_{p,Hf})^2} \quad \text{(A-8)}$$

similar equations has been derived for i=Hf .

The initial and boundary conditions of particles are:

$$t=0\Rightarrow C_{p,i}=0 \text{ , (for breakthrough curve)} \quad \text{(A-9)}$$

$$\frac{\partial C_{p,i}}{\partial r}\Big|_{r=0}=0 \quad \text{(A-10)}$$

$$\varepsilon_p D_{p,i}\frac{\partial C_{p,i}}{\partial r}\Big|_{r=Rp}=k_{f,i}\left(C_i-C_{p,i}\big|_{r=Rp}\right) \quad \text{(A-11)}$$

Bed model

Liquid concentration of each species (i) depends on the particle surface concentration and film mass transfer coefficient which is presented below with respective boundary and initial conditions:

$$\frac{\partial C_i}{\partial t}=-\frac{U_L}{\varepsilon}\frac{\partial C_i}{\partial z}+D_L\frac{\partial^2 C_i}{\partial z^2}- \quad \text{(A-12)}$$

$$\left(\frac{1-\varepsilon}{\varepsilon}\right)\frac{3}{R_p}k_{f,i}\left(C_i-C_{p,i}\big|_{r=Rp}\right)$$

$$t=0\Rightarrow C_i=0 \text{ , (for breakthrough curve)} \quad \text{(A-13)}$$

$$-D_L\frac{\partial C_i}{\partial z}\Big|_{z=0}=\frac{U_L}{\varepsilon}\left(C_{0,i}-C_i\big|_{z=0}\right) \quad \text{(A-14)}$$

$$\frac{\partial C_i}{\partial z}\Big|_{z=L}=0 \quad \text{(A-15)}$$

Finite difference algorithm

Equations (A-7) and (A-12) were rearranged numerically by explicit finite difference method for each species at each point (r_m, z_k, t_n) as following :

At each point of the particle radius (r_m) and each point of the bed (z_k): (i=Zr)

$$\frac{C_{p,Zr}\big|_{m,z,n+1}-C_{p,Zr}\big|_{m,z,n}}{\Delta t}+ \quad \text{(A-16)}$$

$$\frac{1}{F}\frac{(1-\varepsilon_p)}{\varepsilon_p}\times\frac{-b_{Hf}\times q_{m,Zr}b_{Zr}C_{p,Zr}\big|_{m,z,n}}{(1+b_{Zr}C_{p,Zr}\big|_{m,z,n}+b_{Hf}C_{p,Hf}\big|_{m,z,n})^2}\times$$

$$\frac{C_{p,Hf}\big|_{m,z,n+1}-C_{p,Hf}\big|_{m,z,n}}{\Delta t}=$$

$$\frac{1}{F}D_{p,i}\left[\frac{C_{p,Zr}\big|_{m+1,z,n}-2C_{p,Zr}\big|_{m,z,n}+C_{p,Zr}\big|_{m-1,z,n}}{(\Delta r)^2}+\right.$$

$$\left.\frac{2}{r_m}\frac{C_{p,Zr}\big|_{m+1,z,n}-C_{p,Zr}\big|_{m-1,z,n}}{2(\Delta r)}\right]$$

$$F=1+\left[\frac{1-\varepsilon_p}{\varepsilon_p}\right]\frac{q_{m,Zr}b_{Zr}(1+b_{Hf}C_{p,Hf}\big|_{m,z,n})}{(1+b_{Zr}C_{p,Zr}\big|_{m,z,n}+b_{Hf}C_{p,Hf}\big|_{m,z,n})^2} \quad \text{(A-17)}$$

At each point of the bed length (z_k):

$$\frac{C_{Zr}\big|_{k,n+1}-C_{Zr}\big|_{k,n}}{\Delta t}= \quad \text{(A-18)}$$

$$-U_L\left[\frac{C_{Zr}\big|_{k+1,n}-C_{Zr}\big|_{k-1,n}}{2(\Delta z)}\right]+$$

$$D_L\left[\frac{C_{Zr}\big|_{k+1,n}-2C_{Zr}\big|_{k,n}+C_{Zr}\big|_{k-1,n}}{(\Delta z)^2}\right]-$$

$$\left(\frac{1-\varepsilon}{\varepsilon}\right)\frac{3}{R_p}k_{f,Zr}\left(C_{Zr}\big|_{k,n}-C_{p,Zr}\big|_{M,n}\right)$$

$C_{P,Zr}\big|_{M,n}$ = concentration at particle surface

$$C_{p,i}\big|_{m,z,0}=0 \quad \text{(A-19)}$$

$$C_{p,i}\big|_{0,z,n}=C_{p,i}\big|_{1,z,n} \quad \text{(A-20)}$$

$$\varepsilon_p D_{p,i}\frac{C_{p,i}\big|_{M,z,n}-C_{p,i}\big|_{M-1,z,n}}{\Delta r}= \quad \text{(A-21)}$$

$$k_{f,i}\left(C_i\big|_{k,n}-C_{p,i}\big|_{M,n}\right)$$

Bed Initial and boundary conditions:

$$C_i\big|_{k,0}=0 \quad \text{(A-22)}$$

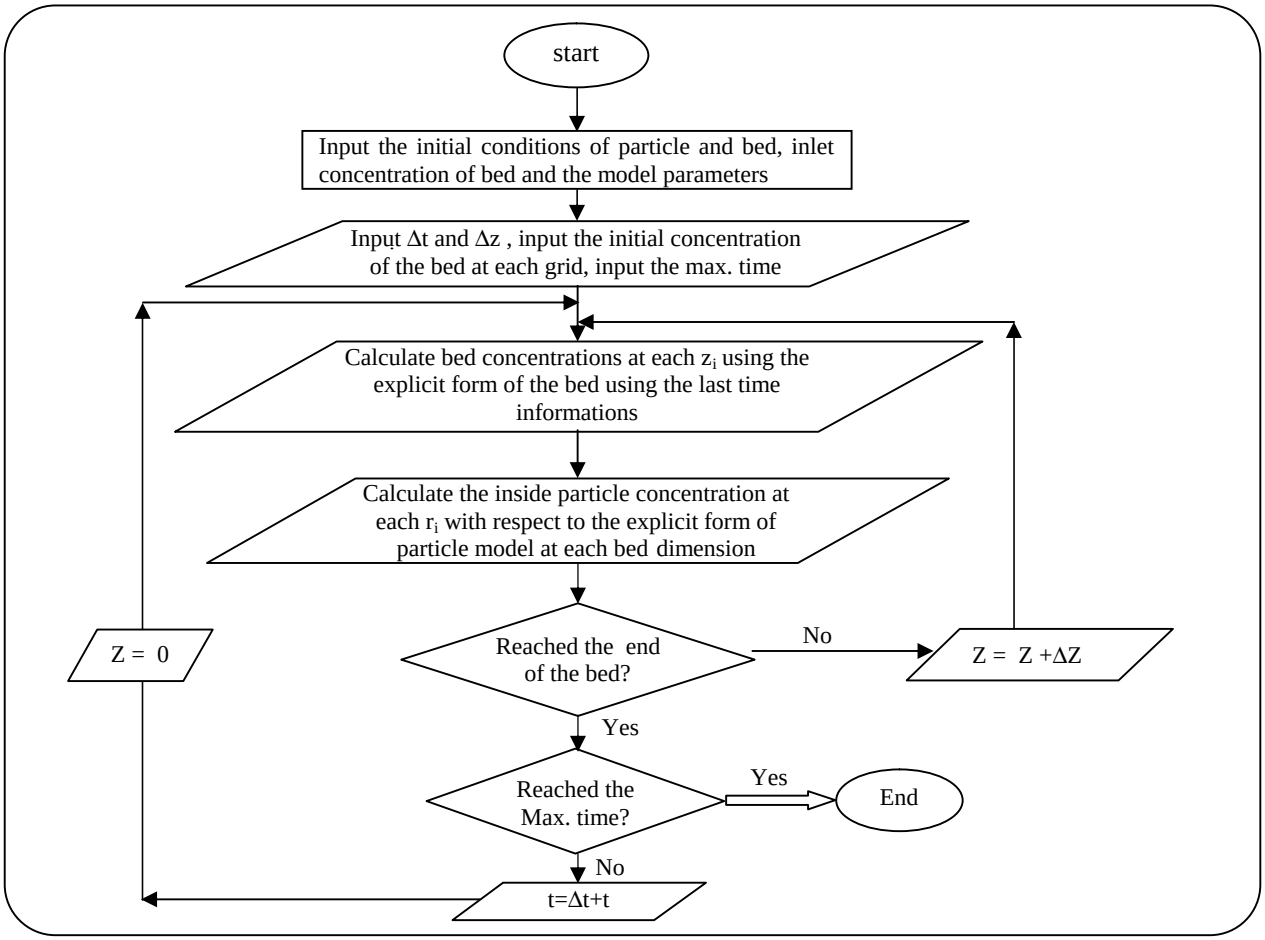

Fig. 7: The flow chart of the numerical solution.

$$-D_L \frac{C_i\big|_{1,n} - C_i\big|_{0,n}}{\Delta z} = U_L\left(C_{i,Feed} - C_i\big|_{0,n}\right) \qquad \text{(A-23)}$$

$$C_i\,|_{K,n} = C_i\,|_{K-1,n} \qquad \text{(A-24)}$$

The general algorithm of numerical solution is presented in Fig. 7.

Acknowledgement

The authors would like to thank Iran National Sciences Foundation (INSF) for their financial support of this project.

Nomenclatures

b	Langmuir constant (mL/ μg)
C	Fluid phase concentration (μg/mL)
C_p	Concentration in liquid inside the pores (μg/mL)
D_m	Molecular diffusion coefficient in solution (m^2/s)
d_p	Particle diameter (m)
D_p	Effective pore diffusion coefficient (m^2/s)
D_L	Axial diffusivity (m^2/s)
k_f	Liquid film mass transfer coefficient (m/s)
H	Column height (m)
q	Resin phase concentration (μg/mL)
q_m	Langmuir constant (μg/mL)
R_p	Particle Radius (m)
t	Time (s)
U_L	Superficial velocity (m/s)
z	Axial distance along column (m)

Greek Symbols

ε	Bed voidage
ε_p	Particle voidage
μ	Fluid viscosity (kg/m s)
ρ	Fluid density (kg/m^3)
τ	Dimensionless time

Received: 12th March 2006 ; Accepted : 14th May 2007

REFERENCES

[1] Byers, C.H. et al., "Zirconium and Hafnium Separation in Chloride Solutions Using Continuous Ion Exchange Chromatography", U.S. Patent, Pat. No. 5, 762,890 (1998).

[2] Gallant, S., Modeling Ion-Exchange Adsorption of Proteins in a Spherical Particle, *J. Chromatography A*, **1028**, 189 (2004).

[3] James, Cowan, Matthew, J. Shaw, The Ion Chromatographic Separation of High Valence Metal Cations Using a Neutral Polystyrene Resin Dynamically Modified with Dipicolonic Acid, *Analyst*, **125**, 2157 (2000).

[4] Ding, X., Mou, S., Retention Behavior of Transition Metals on a Bifunctional Ion-Exchange Column with Oxalic Acid as Eluent, *J. Chromatography A*, **920**, 101 (2001).

[5] Yi, Jia, Gary, L. Foutch, True Multi-Component Mixed-Bed Ion-Exchange Modeling, *Reactive & Functional Polymers*, **60**, 121 (2004).

[6] Jaung, R.S., Kao, H.C., Chen, W., "Column Removal of Ni(II) from Synthetic Electroplating Wastewater Using a Strong-Acid Resin, *Sep. Purif. Tech.*, **49**(1), 36 (2006).

[7] Kostanian, A.E., Modelling Counter-Current Chromatography: A Chemical Engineering Perspective, *J. Chromatography A*, **973**, 39 (2002).

[8] Slizneva, T. E. and Natareev, S. V., Mathematical Modeling of Ion Exchange in an Apparatus with a Fixed Bed of Granular Ion-Exchange Resin, *Theoretical Foundations of Chem. Eng.*, **38** (2), 169 (2004).

[9] Gluszcz, P., Jamroz, T., Sencio, B., Ledakowicz, S., Equilibrium and Dynamic Investigations of Organic Acids Adsorption onto Ion-Exchange Resins", *Bioprocess Biosyst Eng.*, **26**, 185 (2004).

[10] Stuart, R. Gallant, Modeling Ion - Exchange Adsorption of Proteins in a Spherical Particle, *J. Chromatography A*, **1028**, 189 (2004).

[11] Hamid Feizy Zarnagh, Modeling and Effective Parameters Estimation in Separation of Ziconium and Hafnium Cations by Ion Exchange Resin, MSc. Thesis ,Chem. Eng. Division., University of Tehran, (2006).

[12] Kalantari, M., Investigation of Zr (IV) and Hf (IV) Separation from Aqueous Solution by Ion Exchange Chromatographic Method, MSc Thesis ,Chem. Eng. Division, University of Tehran, (2005)

[13] Slatter, M. J., "Principles of Ion Exchange Technology", Butterworth- Heinemann, p. 31 (1991).

[14] Olieslager, W. D'. and Comeyne, D., Properties of Zr(IV) and Hf(IV) Ions on Dowex 50 W X8: An Ion Exchange Equilibrium Study, *React. Polym.*, **7**, 133 (1988).